

## **ITERATIVE HYBRID METHOD FOR ELECTROMAGNETIC SCATTERING FROM A 3-D OBJECT ABOVE A 2-D RANDOM DIELECTRIC ROUGH SURFACE**

**W. Yang, Z. Q. Zhao<sup>\*</sup>, C. H. Qi, W. Liu, and Z. P. Nie**

School of Electronic Engineering, University of Electronic Science and Technology of China, Chengdu 611731, China

**Abstract**—An iterative hybrid method combining the Kirchhoff approximation (KA) and the multilevel fast multipole algorithm (MLFMA) is studied for electromagnetic scattering from a three-dimensional (3-D) object above a two-dimensional (2-D) random dielectric rough surface. In order to reduce the computational costs, some treatments have been studied. Firstly, the fast far-field approximation (FAFFA) is utilized to speed up the electromagnetic coupling interaction process between the rough surface and the object. Secondly, based on the scattering mechanism of the rough surface, a truncation rule on moderate rough surface for bi-static scattering is proposed under the plane wave illumination, which can further speed up the iteration. Compared with the conventional methods, the hybrid method with the above treatments is very efficient to analyze the scattering of a 3-D object above random rough surfaces. Simulation results validate the effectiveness and accuracy of the iterative hybrid method.

### **1. INTRODUCTION**

The study of electromagnetic (EM) scattering from the composite model of a three-dimensional (3-D) object over a two-dimensional (2-D) rough surface has been of great interest in recent years. It is a typical problem in the study of EM scattering characteristics of an object underlying its environment, such as ships on the sea, tanks on the ground, et al.. Some previous studies have focused on the half-space Green's function model [1]. However, the half-space Green's function

---

*Received 30 April 2011, Accepted 13 June 2011, Scheduled 16 June 2011*

\* Corresponding author: Zhiqin Zhao (zqzhao@uestc.edu.cn).

model simplifies the scattering problem of the rough surface. Some works degraded this 3-D problem to a 2-D problem, i.e., simplified the 3-D model to a model with 2-D object over one-dimensional (1-D) rough surface [2–4]. However, this simplified model is not a realistic scattering model in engineering.

Numerous methods have been approached in the scattering of the composite model. In [5], an iterative numerical algorithm was applied to calculate the scattering of the composite model, where a “four-path” model was introduced to illustrate the interaction mechanism between the interesting target and the rough surface environment. Based on the “four-path” model, Jin and Ye [6] introduced the analytical-numerical hybrid algorithm for a 2-D object above a 1-D rough surface, and the length truncation rule for 1-D case was discussed. It can solve the scattering problem of the 1-D rough surface. But it is hard to efficiently deal with the problem of the 2-D rough surface because of the expensive interaction time. Recently, the asymptotic method [7, 8] was introduced to calculate the scattering of the 3-D composite model. The asymptotic method can give good results under certain cases since the multiple scattering effects have been taken into account. But it can work well only when the target does not have complicated structure. In [9], the parallel FDTD was used to study the 3-D composite model. Owing to its own drawback in dealing with surface problem, the FDTD is not enough efficient for this 3-D composite model problem, especially when the sea surface is EM large scale.

In this paper, an iterative hybrid method is introduced to analyze the composite model of a 3-D object over a 2-D rough surface. This method is consisted of the Kirchhoff approximation (KA) [10] and the multilevel fast multipole algorithm (MLFMA) [11, 12]. The KA has been widely applied to calculate the scattering of the rough surface, since the induced current distribution can be easily obtained by the physical optics approximation with the very low computational cost. As a rigorous method, the MLFMA has been applied to calculate the scattering of the arbitrary-shaped target. It reduces the computational costs to  $o(N \log N)$  ( $N$ : the number of unknowns) instead of the order  $o(N^2)$  of the method of moment (MoM) [2]. Up to now, it has been regarded as one of the most efficient methods among the numerical methods.

Therefore, we combined the advantages of the KA and MLFMA in the hybrid method. In order to make it more efficient, a rule for 2-D truncated rough surface area in bi-static scattering problem is proposed under the plane wave illumination based on the scattering mechanism of the rough surface. Meanwhile, the fast far-field approximation (FAFFA) [13] for the hybrid method is applied to speed up the

electromagnetic coupling interaction process. This method can greatly reduce the computational costs, including both RAM memory and CPU time.

## 2. ITERATIVE MODEL OF ANALYTICAL-NUMERICAL METHODS

The scattering model of a 3-D object above a 2-D random dielectric rough surface is approached in this section. The isotropic Gaussian spectrum [14] is used to simulate the rough surface. The rough surface height is noted as  $\zeta(x, y)$ . Its mean is  $\langle \zeta(x, y) \rangle = 0$ . The correlation lengths  $l_x$  and  $l_y$  in the  $x$  and  $y$  directions are assumed to be  $l_x = l_y = l_c$ .

Figures 1 and 2 show the “four-path” scattering model [5, 6]. The 1st path is the incident wave  $\vec{E}^i(\vec{r})$  illuminating on the object which gives a scattered field, the 2nd path is the  $\vec{E}^i(\vec{r})$  illuminating on the rough surface which gives a scattered field, the 3rd path is the current distribution on the object induced by  $\vec{E}^i(\vec{r})$  gives a mutual scattered field  $\vec{E}_o^s(\vec{r})$  to the rough surface, on which an extra current is induced and gives rise to another scattered field, and the 4th path is the current distribution on the rough surface induced by  $\vec{E}^i(\vec{r})$  give a mutual scattered field  $\vec{E}_s^s(\vec{r})$  to the object, on which an extra current is induced and brings another scattering.

The scattering of the composite model is solved in an iterative process. The interactions between the object and rough surface are accounted by updating the excitation fields including the field  $\vec{E}_o^{i(n)}(\vec{r})$  on the object and the field  $\vec{E}_s^{i(n)}(\vec{r})$  on the rough surface. The updating

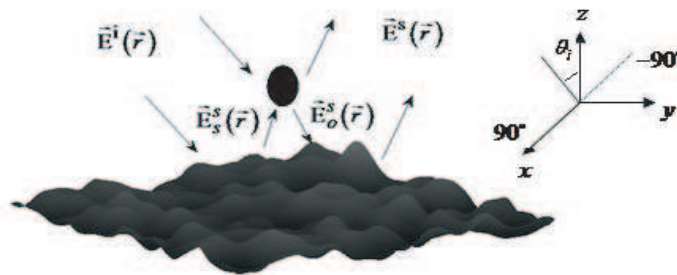
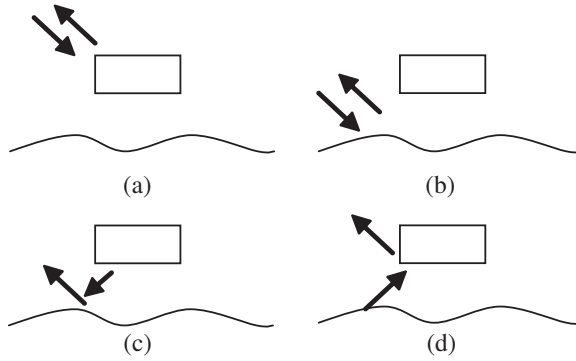


Figure 1. The schematic diagram of scattering model.



**Figure 2.** The “four-path” scattering model. (a) Path 1. (b) Path 2. (c) Path 3. (d) Path 4.

processes are expressed as

$$\vec{E}_s^{i(n)}(\vec{r}) = \vec{E}^i(\vec{r}) + \vec{E}_o^{s(n-1)}(\vec{r}) \quad (r \in \mathbb{Z}), \tag{1a}$$

$$\vec{E}_o^{i(n+1)}(\vec{r}) = \vec{E}^i(\vec{r}) + \vec{E}_s^{s(n)}(\vec{r}) \quad (r \in \mathbb{Z}'), \tag{1b}$$

where  $n = 1, 2, \dots$  denotes the  $n$ -th iterative step, at the first step, i.e.,  $n = 1$ ,  $\vec{E}_s^{i(1)}(\vec{r}) = \vec{E}^i(\vec{r})$ . And the  $\mathbb{Z}$  and  $\mathbb{Z}'$  stand for the rough surface area and the object surface area, respectively.

According to the Huygen’s principle, the scattering field  $\vec{E}_s^{s(n)}(\vec{r})$  of the dielectric rough surface can be obtained by

$$\begin{aligned} \vec{E}_s^{s(n)}(\vec{r}) = & \iint_{\mathbb{Z}} j\omega\mu_0 \vec{G}(\vec{r}, \vec{r}') \cdot \hat{n} \times \vec{H}_s^{tot(n)}(\vec{r}') \\ & + \nabla \times \vec{G}(\vec{r}, \vec{r}') \cdot \hat{n} \times \vec{E}_s^{tot(n)}(\vec{r}') dS', \end{aligned} \tag{2}$$

in which  $\vec{G}(\vec{r}, \vec{r}')$  is the dyadic Green’s function in free space,  $\vec{H}_s^{tot(n)}$  and  $\vec{E}_s^{tot(n)}$  are the total fields corresponding to the polarization of incident wave and its reflect characteristic,  $\hat{n}$  denotes the outer normal vector of the scattering surface. The integration  $dS'$  is on the surface area  $\mathbb{Z}$ .

The scattered field  $\vec{E}_o^{s(n)}(\vec{r})$  from the object due to its current distribution  $\vec{J}_o^{(n)}(\vec{r}')$  can be expressed in terms of the electric field integral equation (EFIE) as

$$\vec{E}_o^{s(n)}(\vec{r}) \Big|_{\text{tan}} = \left[ j\omega\mu_0 \iint_{\mathbb{Z}'} \vec{G}_0(\vec{r}, \vec{r}') \cdot \vec{J}_o^{(n)}(\vec{r}') dS' \right]_{\text{tan}}, \tag{3}$$

where the subscript “tan” denotes the tangential component of the field. It can be solved by using the MLFMA (see the details in [11, 12]), the interactions between the elements are classified as near-region and the far-region. The near-region matrix elements are calculated directly using the method of moment (MoM) [2] and the far-region elements are acquired by using MLFMA engine. The integration  $dS'$  is on the target area  $Z'$ .

Once the iterative process begins, a positive constant defined as  $v = |\vec{J}_o^{(n)} - \vec{J}_o^{(n-1)}|/|\vec{J}_o^{(n)}|$  is used to control the convergence in this model. If the  $v$  is less than a threshold (for example, 0.001), the interaction process is assumed to reach a stable state and will stop. Then the scattering field can be calculated through the stable current distributions both on the rough surface and on the target.

In the first experiment of this paper, the hybrid method was used to calculate the scattering from the composite model of a cube  $a = 2.0\lambda$  long located at  $h = 3.0\lambda$  above a rough surface of size  $30\lambda \times 30\lambda$ , whose root mean square height ( $hrms$ ) is  $0.2\lambda$ , and the correlation length  $l_c$  is  $1.5\lambda$ , while the curvature radius  $\rho$  is  $6\lambda$ . The electromagnetic frequency is 10 GHz. The incident angle is  $(30^\circ, 0^\circ)$ . For the Monte Carlo study, the results were averaged over 20 realizations. The bi-static radar cross section (RCS:  $\sigma$ ) results of the composite model for the horizontal polarization ( $HH$ ) and the vertical polarization ( $VV$ ) are shown in Fig. 3. The dashed lines are the results for MLFMA, which are used as references in this paper. It shows that the hybrid method works well for  $HH$  polarization and  $VV$  polarization at the moderate scattering angles ( $|\theta_s| \leq 70^\circ$ ). For  $HH$  polarization, when the forward scattering angle is larger than  $70^\circ$ , the agreement decreases.

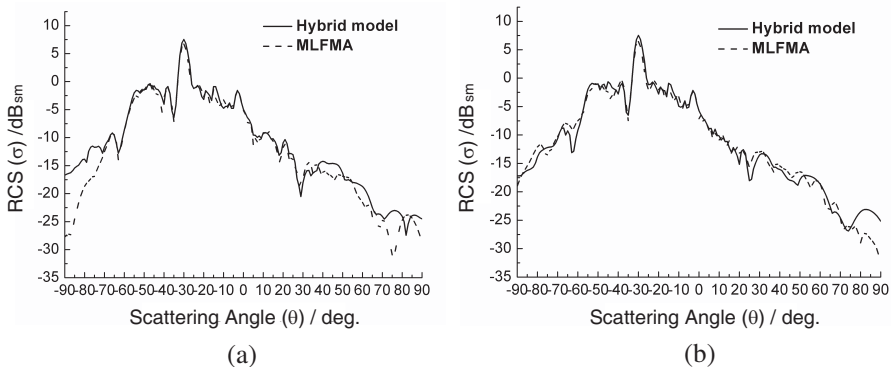


**Figure 3.** The comparisons between the iterative hybrid method and MLFMA. (a)  $HH$  polarization. (b)  $VV$  polarization.

In order to quantitatively describe the goodness of fit, the relative error (RE:  $\zeta$ ) is introduced and expressed in (4)

$$\zeta = \frac{\sum_{i=1}^N |x_i - y_i|}{\sum_{i=1}^N |x_i|} \times 100\%, \quad (x_i : \text{ref. data}, y_i : \text{calc. data}), \quad (4)$$

In the scattering angles (from  $-70^\circ$  to  $70^\circ$ ), which is usually regarded as moderate angles, the error is less than 8% for  $HH$  polarization and 7% for  $VV$  polarization. The error is mainly because that KA is used to calculate the scattering of the surface in the hybrid method. KA is subjected to the shading effect, which is even worse when the angle tends to grazing. However, the hybrid model still works well for most of the scattering angles, especially for moderate angles.

### 3. SPECIAL TREATMENTS IN THE HYBRID METHOD

For the EM scattering simulation from the composite model, Johnson [5] proposed the difference field radar cross section (d-RCS) as the difference scattering field between the object/surface and the surface only. Here, the scattering field directly from the rough surface is subtracted from the total scattering field of the composite model. The d-RCS contains the scattering contributions from the target and multiple interactions between the target and the rough surface environment. For the multiple interactions between the two scattering objects, the amplitude of interaction attenuates with the increasing distance  $R$  ( $R = |\vec{r} - \vec{r}'|$ ,  $\vec{r}$  and  $\vec{r}'$  are the points on the  $\mathbb{Z}$  and the  $\mathbb{Z}'$ , respectively) according to the scalar Green's function  $G = e^{-jkR}/R$ . Therefore, the integral area can be truncated at a limited surface according to the required precision.

Different from the numerical method, the analytical-numerical hybrid model will not bring the electromagnetic edge effects, that is to say, the tapered EM window [14] will be unnecessary. Compared with the tapered wave illumination, the plane wave illumination needs much less calculation area for the same effective scattering area. Therefore, this paper focuses on the plane wave illumination problem.

#### 3.1. Truncation Rule for Rough Surface

Obviously the scattering field from rough surface is significantly decreasing at the far edges of the rough surface. For the d-RCS calculation, it is useless and unnecessary to consider the contribution

of the unlimited rough surface. The integral area can be truncated for required precision according to the truncation rule.

Jin and Ye [6] gave a principle of truncated length for the 1-D surface, the rule originates from the decrease in the tangential component of the field at the field point  $\vec{r}$  on the rough surface with the increasing distance  $R$  in the Green's function. It can be extended to 2-D case. The truncated surface length  $L_x$  and  $L_y$  in  $x$  and  $y$  directions can be truncated as

$$L_x \geq 2Z_0 \sqrt{\xi^{-4/3} - 1} + lx, \tag{5a}$$

$$L_y \geq 2Z_0 \sqrt{\xi^{-4/3} - 1} + ly, \tag{5b}$$

where  $\xi$  is a small positive constant to control the precision of the error of truncated Green's function, (usually it is set to 0.01). And  $Z_0$  denotes the height of the top point of target from the sea surfaces,  $lx$  and  $ly$  are the object geometric size in  $x$  and  $y$  directions, respectively.

Though this principle can ensure enough precision, it brings huge computation time in the iterative process because of the large scale surface area. Based on the specular reflection properties of the moderate rough surfaces [15], (generally for  $hrms \leq 1\lambda$ ), the interaction between the object and the rough surface can be calculated within a smaller truncated area.

The specular reflection properties in the scattering from rough surfaces have been demonstrated [6, 9]. The amplitude of its scattering field at the specular direction is higher up to 10 dB than the scatterings at other directions, which implies that the main scattering energy concentrates at the specular direction. Therefore, the integral surface area can be truncated according to the specular reflection.

Figure 4 illustrates the specular reflection scheme for 1-D case. (The principle for 2-D case is straight forward). Suppose the object

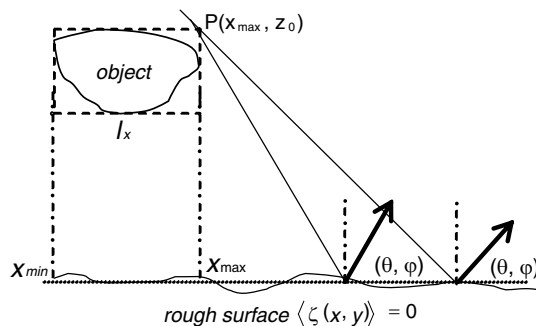


**Figure 4.** The 1-D specular reflection schema.

is located in a fictitious box noted as the dashed line rectangle in the figure. Its highest point is the  $P(x, y, z_0)$ . According to the geometry ray-tracing method, the truncated length of the rough surface is determined by

$$x_1 = x_{\min} - Z_0 \tan \theta, \quad (6a)$$

$$x_2 = x_{\max} + Z_0 \tan \theta, \quad (6b)$$

Therefore, the surface length can be truncated at  $Lx = x_2 - x_1 = 2z_0 \tan \theta + lx$  ( $lx = x_{\max} - x_{\min}$ ). Similarly, the size of rough surface in the  $y$  direction is described as

$$y_1 = y_{\min} - Z_0 \tan \theta, \quad (7a)$$

$$y_2 = y_{\max} + Z_0 \tan \theta, \quad (7b)$$

It should be noted that the above scheme is suitable for the incident or scattering angle  $(\theta, \varphi)$ . Different angles will have different truncated areas. In order to simplify the statement, the rules given by Eqs. (6) and (7) are noted as an operator  $\Lambda(\theta, \varphi)$ . Different from the mono-static scattering case [16], the regions for bi-static scattering are jointly determined by the incident angle  $(\theta_i, \varphi_i)$  and the scattering angle  $(\theta_{sn}, \varphi_{sn})$  (the subscript of  $n$  denotes the  $n$ -th scattering angle). Therefore, the regions  $S$  for the bi-static scattering are represented as

$$S = \Lambda(\theta_i, \varphi_i) \cup (\Lambda(\theta_{s1}, \varphi_{s1}) \cup \Lambda(\theta_{s2}, \varphi_{s2}) \cup \dots \cup \Lambda(\theta_{sn}, \varphi_{sn})), \quad (8)$$

The Eq. (8) can be simply equivalent to the operator  $\Lambda(\theta_m, \varphi_m)$  at the largest scattering angle  $(\theta_m, \varphi_m)$ . Its efficiency of the new truncation rule can be demonstrated by an example of a delta current source  $\delta(r')$  at  $r' = (0, 0, z_0)$ . Different truncated areas have been obtained according to the different scattering angles. The truncation rule proposed in this paper is more flexible than the Jin's rule.

The truncated areas for different largest angles  $\theta_m$  of  $70^\circ$ ,  $75^\circ$ ,  $80^\circ$ ,  $85^\circ$  have been compared in Table 1. Obviously, the truncated areas using the rule proposed in this paper are less than the truncated area using Jin's rule. Even for the  $85^\circ$  case, the truncated surface area obtained by the rule in this paper is 70% less than that by Jin's rule. The accuracy by using the proposed truncation rule will be further studied in the following section.

**Table 1.** The comparison on the truncated areas for the different rules.

$\theta_m$	<i>Proposed Rule</i>				<i>Jin's Rule</i>
	$70^\circ$	$75^\circ$	$80^\circ$	$85^\circ$	
Truncated Area ( <i>normalized by <math>z_0 * z_0</math></i> )	30.2	55.7	129	523	1853

### 3.2. Acceleration Technique Using FAFFA

Iterative process is another high cost of time consuming, especially for Monte Carlo simulations in the large composite model, therefore it is necessary to accelerate the interaction solution. Borrowing the idea from the fast far-field approximation (FAFFA) [13] in the MLFMA, the coupling interaction between KA and MLFMA can be accelerated in the interaction between far-field region groups. Once the induced current distributions have been solved by the analytical or numerical methods, the mutual scattered field can be calculated through the Green's function. Supposed that  $\vec{r}_i$  is an observation point located in an observation group  $m$ , and  $\vec{r}_j$  is a source point that is located in a source group  $n$ .  $\vec{r}_m$  and  $\vec{r}_n$  represent the centers of the observation and the source groups. Under the far-field condition, i.e.,  $|\vec{r}_{im} + \vec{r}_{nj}| \gg |\vec{r}_{mn}|$ , the Green's function can be approximated as

$$\frac{e^{ik|\vec{r}_i - \vec{r}_j|}}{|\vec{r}_i - \vec{r}_j|} = \frac{e^{ik|\vec{r}_{im} + \vec{r}_{mn} + \vec{r}_{nj}|}}{|\vec{r}_{im} + \vec{r}_{mn} + \vec{r}_{nj}|} \approx \frac{e^{ikr_{mn}} e^{ik\hat{\mathbf{r}}_{mn} \cdot (\vec{r}_{im} + \vec{r}_{nj})}}{|\vec{r}_{mn}|}, \quad (9)$$

where  $\hat{\mathbf{r}}_{mn}$  is the unit vectors from group  $n$  to group  $m$ .

The interactions between the elements are classified as the near region and the far region. The near-region interaction is solved directly, and the far-region interaction is speeded up by the FAFFA. Suppose there are  $C_1$  and  $C_2$  basis functions in each object group and in each rough surface group, respectively, the consumed time in the interaction process can be reduced to  $o(MN)/(C_1 C_2)$ , even to  $o(\sqrt{MN})$  if  $C_1 \sim \sqrt{M}$  and  $C_2 \sim \sqrt{N}$ ,  $M$  and  $N$  denote the number of the unknowns of object and rough surface, respectively. Similar to the MLFMA, the finest length of each group in the rough surface groups is set to  $0.3\lambda \sim 0.5\lambda$ . Usually most of the interactions between the object groups and the rough surface groups satisfy the far-field condition for very large rough surface. Therefore, it can greatly speed up the electromagnetic interaction process.

## 4. SIMULATIONS AND DISCUSSIONS

Consider an example, a cube with  $3\lambda$  in length is located at  $h = 10\lambda$  high above a rough perfect electric conducting (PEC) surface with  $hrms = 1\lambda$ ,  $l_c = 1.5\lambda$ ,  $\rho = 4\lambda$ . Set the incident angle as  $(\theta_i = 40^\circ, \varphi_i = 0^\circ)$ , and setting the largest scattering angles as  $\theta_m = 70^\circ$  and  $80^\circ$ , respectively. According to the truncation rule described in Section 3, the truncated areas are  $S_{(\theta_m=70^\circ)} = 55\lambda * 55\lambda$ ,  $S_{(\theta_m=80^\circ)} = 113\lambda * 113\lambda$ . And the truncated area using the Jin's rule ( $\xi = 0.01$ ) is  $S = 433\lambda * 433\lambda$ , which is considered as the reference result again. The

total consuming time for the three truncated surface are about 4324 s, 11921 s, 138192 s for  $HH$  polarization, and 4301 s, 11778 s, 135312 s for  $VV$  polarization, respectively. It is a big improvement in the total time costs. The comparison on the bi-static difference field radar cross section (d-RCS) is shown in Fig. 5. From the comparisons between  $HH$  and  $VV$  polarizations, the results using the proposed rule match very well with the reference result. There are some deviations for the  $\theta_m = 70^\circ$  case at the scattering angles of  $\theta > 70^\circ$ , and some deviations for the  $\theta_m = 80^\circ$  case at the scattering angles of  $\theta > 80^\circ$ , which demonstrates the truncation rule in the above analysis. Within the scattering angles (from  $-80^\circ$  to  $80^\circ$ ), the relative error is less than 8% and 7% at the  $70^\circ$  and  $80^\circ$  cases respectively for  $HH$  polarization, and less than 6% and 4% at the  $70^\circ$  and  $80^\circ$  cases respectively for  $VV$  polarization. Therefore, the truncated area can be set according to the domain of the scattering angles. The truncated surface area is much less than the previous size even for a large angle case (for example:  $85^\circ$ ).

As another example, suppose an airplane model with 6.0 m long and 4.5 m wide in the wing locating at  $h = 6.0$  m above the random rough sea surface. The geometric model of the model is shown in Fig. 6(a). The geometry parameters for the model are given in Fig. 6(b). For the rough surface, the parameters are  $hrms = 0.3\lambda$ ,  $l_c = 1\lambda$ ,  $\rho = 5\lambda$ . According to the proposed truncation rule, the truncated area is  $43 \text{ m} \times 44.5 \text{ m}$  (about  $143\lambda \times 148\lambda$ ) by setting  $\theta_m = 70^\circ$ . And the EM frequency is 1.0 GHz, the complex relative permittivity of the sea water at this frequency is  $(72.7664, -84.521)$  when the temperature is  $20^\circ$  and the salinity is  $32.54\text{‰}$ . The incident angle is set to  $(30^\circ, 90^\circ)$ .

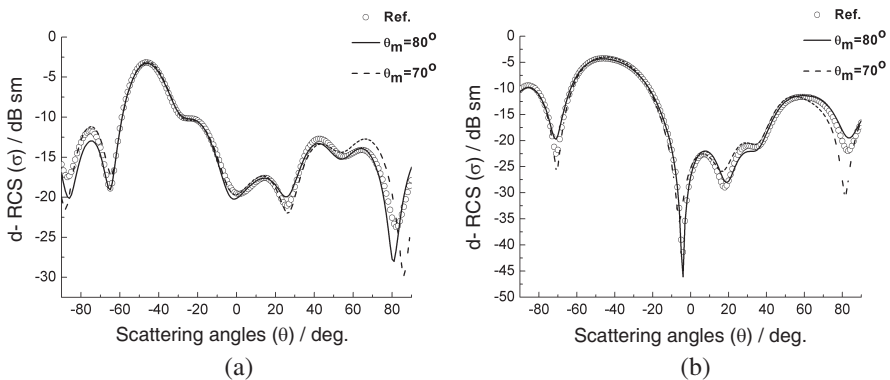


**Figure 5.** The comparison of d-RCS for the two truncated areas. (a)  $HH$  polarization. (b)  $VV$  polarization.

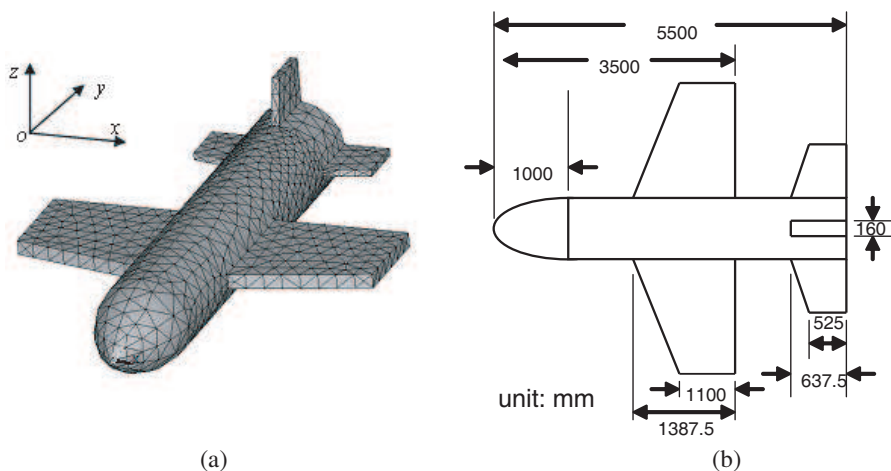


**Figure 6.** An airplane example. (a) 3-D model with the triangular surface mesh. (b) In the top view.

The number of the total triangular meshing patches for the airplane model is 67352, and the number of the unknowns is 101028 with the Rao-Wilton-Glisson (RWG) basis function [17], the total consumed memory 405.4 MB for each realization. The total number of the triangular meshing patches for the rough surface is about 4300000. For the composite model, it can be solved well in a common PC machine using the hybrid method and FAFFA.

For the Monte Carlo study, the results are averaged over 20 realizations. With the hybrid algorithm and FAFFA acceleration technique, the results of bi-static d-RCS with (or without) sea background scattering are given in the Fig. 7. The sea scattering background will change the scattering properties of targets, especially in the spatial ranges of low scattering energy. At some spatial directions, the scattering field is significantly enhanced up to 20 dB.

For the FAFFA acceleration technique, its efficiency can be estimated through the basis functions in the each object group and rough surface group,  $C_1$  and  $C_2$ , as aforementioned. Generally, it will speed up more than (estimated) 100 times for each realization compared with direct interaction. Without doubt, the hybrid method with FAFFA is a very useful tool to analyze the scattering of targets above the rough surfaces.

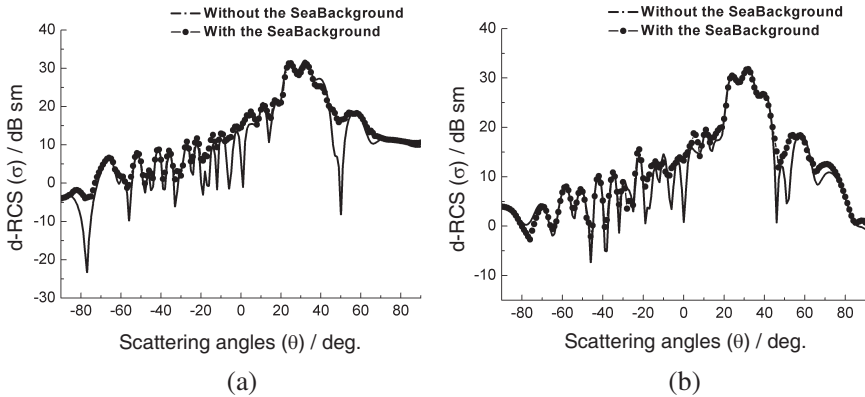


**Figure 7.** The d-RCS comparison in the bi-static scattering case. (a)  $HH$  polarization. (b)  $VV$  polarization.

## 5. CONCLUSIONS

In this paper, a hybrid method combining the KA and MLFMA is used to solve the composite model of an object over a random rough surface. Meanwhile the fast far-field approximation (FAFFA) technique was applied to speed up the electromagnetic interaction between the object and the rough surface. Based on the specular reflection properties of the moderate rough surfaces, a truncation rule under the plane wave illumination has been proposed. It greatly reduces the truncated areas compared with Jin's method at a moderate rough surface with a very good precision. Through the above experiments, it has been demonstrated that this method can not only give the reliable results, but also reduces the computational memory requirements and consumed time hugely compared with conventional numerical methods.

One thing needed to be pointed out is that we assumed the surface be Gaussian surface in the simulation, while the representation of a realistic sea surface is usually described by a P-M (Pierson-Moskowitz) spectrum [18]. Under this condition, because the curvature radius  $\rho$  of PM surface is smaller, the modifications for the traditional KA are necessary. This will be studied in our further work.

## ACKNOWLEDGMENT

This work is supported in part by the NSFC (No. 60927002) and the National High-Tech Research and Development Program of China (863 Program, No. 2007AA12Z159).

## REFERENCES

1. Liu, Z. J. and L. Carin, "Efficient evaluation of the half-space Green's function for fast-multipole scattering models," *Microw. Opt. Technol. Lett.*, Vol. 29, No. 6, 388–392, 2001.
2. Guo, L. X., A. Q. Wang, and J. Ma, "Study on EM scattering from 2-D target above 1-D large scale rough surface with low grazing incidence by parallel MoM based on PC clusters," *Progress In Electromagnetics Research*, Vol. 89, 149–166, 2009.
3. Wang, X. and L. W. Li, "Numerical characterization of bistatic scattering from pec cylinder partially embedded in a dielectric rough surface interface: Horizontal polarization," *Progress In Electromagnetics Research*, Vol. 91, 35–51, 2009.
4. Wang, X., Y. B. Gan, and L. W. Li, "Electromagnetic scattering by partially buried PEC cylinder at the dielectric rough surface interface: TM case," *IEEE Antennas and Wireless Propagation Letters*, Vol. 2, 2003.
5. Johnson, J. T., "A numerical study of scattering from an object above a rough surface," *IEEE Trans. Antennas Propag.*, Vol. 50, No. 10, 1361–1367, 2002.
6. Ye, H. X. and Y. Q. Jin, "A hybrid analytic-numerical algorithm of scattering from an object above a rough surface," *IEEE Trans. Geosci. Remote Sens.*, Vol. 45, No. 5, 1174–1180, 2007.
7. Baussard, A., M. Rochdi, and A. Khenchaf, "PO/MEC-based scattering model for complex objects on a sea surface," *Progress In Electromagnetics Research*, Vol. 111, 229–251, 2011.
8. Xu, F. and Y. Q. Jin, "Bidirectional analytic ray tracing for fast computation of composite scattering from electric-large target over a randomly rough surface," *IEEE Trans. Antennas Propag.*, Vol. 57, No. 5, 1495–1505, 2009.
9. Guo, L. X. and H. Zeng, "Bistatic scattering from a three dimensional object above a two dimensional randomly rough surface modeled with the parallel FDTD approach," *J. Opt. Soc. Am.*, Vol. 26, No. 11, 2383–2392, 2009.
10. Thorsos, E. I., "The validity of the Kirchhoff approximation for rough surface scattering using a gaussian roughness spectrum," *J. Acoust. Soc. Am.*, Vol. 83, No. 1, 78–92, 1988.
11. Yang, W., Z. Q. Zhao, and Z. P. Nie, "Fast fourier transform multilevel fast multipole algorithm in rough ocean surface scattering," *Electromagnetics*, Vol. 29, No. 7, 541–552, 2009.
12. Taboada, J. M., M. G. Araujo, J. M. Bertolo, L. Landesa, F. Obelleiro, and J. L. Rodriguez, "MLFMA-FFT parallel algo-

- rithm for the solution of large-scale problems in electromagnetics,” *Progress In Electromagnetics Research*, Vol. 105, 15–30, 2010.
13. Chew, W. C., T. J. Cui, and J. M. Song, “A FAFFA-MLFMA algorithm for electromagnetic scattering,” *IEEE Trans. Antennas Propag.*, Vol. 50, No. 11, 1641–1648, 2002.
  14. Thorsos, E. I. and D. R. Jackson, “The validity of the perturbation approximation for rough surface scattering using a gaussian roughness spectrum,” *J. Acoust. Soc. Am.*, Vol. 86, No. 1, 261–277, 1989.
  15. Ye, H. X. and Y. Q. Jin, “Fast iterative approach to difference scattering from the target above a rough surface,” *IEEE Trans. Geosci. Remote Sens.*, Vol. 44, No. 1, 108–115, 2006.
  16. Zhang, X. Y. and X. Q. Sheng, “Highly efficient hybrid method for computing the backscattering from objects above a dielectric rough surface,” *Transactions of Beijing Institute of Technology*, Vol. 30, No. 4, 460–463, 2010 (in Chinese).
  17. Rao, S. M., D. R. Wilton, and A. W. Glisson, “Electromagnetic scattering by surfaces of arbitrary shape,” *IEEE Trans. Antennas Propag.*, Vol. 30, No. 3, 409–418, 1982.
  18. Pierson, W. and L. Moskowitz, “A proposed spectral form for fully developed wind seas based upon the similarity theory of S. A. Kitaigorodskii,” *Journal of Geophysical Research*, Vol. 69, 5181–5190, 1964.